physica status solidi

pss

www.interscience.wiley.com

reprints

WILEY-VCH

REPRINT

Phys. Status Solidi B **246**, No. 6, 1318–1326 (2009) / **DOI** 10.1002/pssb.200844492

physica status solidi b
www.pss-b.com
basic solid state physics

Luminescence of dimer lead centers in aluminium perovskites and garnets

V. Babin[1], V. Bichevin[1], V. Gorbenko[2], A. Makhov[1], E. Mihokova[3], M. Nikl[3], A. Vedda[4], S. Zazubovich[*,1], and Yu. Zorenko[2]

[1] Institute of Physics, University of Tartu, Riia 142, 51014 Tartu, Estonia
[2] Ivan Franko National University of Lviv, Gen. Tarnavsky 107, 79017 Lviv, Ukraine
[3] Institute of Physics AS CR, Cukrovarnicka 10, 162 53 Prague, Czech Republic
[4] Dipartimento di Scienza dei Materiali, Università di Milano-Bicocca, Via Cozzi 53, 20125 Milano, Italy

Received 26 December 2008, revised 2 February 2009, accepted 18 February 2009
Published online 26 March 2009

PACS 71.55.Ht, 78.47.–p, 78.55.Hx

[*] Corresponding author: e-mail svet@fi.tartu.ee, Phone: +3727 374 766, Fax: +3727 383 033

Steady-state emission and excitation spectra and luminescence decay kinetics were studied at 80–300 K under excitation in the 2.5–6.0 eV energy range for undoped and Ce^{3+}-doped aluminium garnet ($Lu_3Al_5O_{12}$, $Y_3Al_5O_{12}$) and aluminium perovskite ($LuAlO_3$, $YAlO_3$) single crystalline films (SCF) grown by Liquid Phase Epitaxy method from the PbO-based flux. The aim of the work was to identify spectral bands, arising from lead-induced centers of different types, and to clarify their influence on scintillation characteristics of Ce^{3+} centers. It was found that in the perovskite SCF studied, the concentration of single Pb^{2+}-based centers is comparatively small. In the SCF of garnets, in YAG SCF their concentration is considerably smaller than in LuAG SCF. The lead-induced emission at about 3.1–3.2 eV excited around 3.9 eV was observed in all the SCF studied and ascribed to the dimer lead centers of the type of {Pb^{2+} – oxygen vacancy – Pb^{2+}}. In Ce^{3+}-doped perovskite SCF, due to a strong overlap of the excitation band of the dimer centers and the emission band of Ce^{3+} centers, a considerable influence of dimer lead centers on the scintillation characteristics of these materials is expected. In the SCF of garnets, the influence of dimer lead centers on the characteristics of Ce^{3+} centers is negligible.

1 Introduction Single crystals of lutetium–aluminium garnet $Lu_3Al_5O_{12}$ (LuAG), yttrium–aluminium garnet $Y_3Al_5O_{12}$ (YAG), lutetium–aluminium perovskite $LuAlO_3$ (LuAP), and yttrium–aluminium perovskite $YAlO_3$ (YAP), doped with Ce^{3+} ions, have a high density and excellent mechanical and chemical stability, possess an intense and fast emission due to 5d–4f radiative transition of Ce^{3+} and have been, thus, considered for fast scintillator applications (see, e.g., [1–4]). Under excitation of the undoped, melt-grown bulk single crystals (SC) in the band-to-band and exciton energy range, an intense complex slow intrinsic luminescence was observed in the UV spectral range. Such emissions were ascribed to the exciton localized near the Lu_{Al}^{3+} or Y_{Al}^{3+} antisite defects [5–7] and to the antisite defects themselves [8]. The presence of such defects in the garnet and perovskite structures was predicted also by theoretical calculations [9–12] and the ability of such defects to create shallow electron traps was recently theoretically examined in YAP [13]. As this intrinsic emission is overlapped with the Ce^{3+} absorption bands, the scintillation response of the Ce^{3+}-doped materials can be negatively affected due to the appearance of a considerable amount of slow decay components [5, 14].

In [5, 8] it was found that the concentration of antisite defects is strongly suppressed in single crystalline films (SCF) grown by the Liquid Phase Epitaxy (LPE) method, and the Ce^{3+}-doped SCF show considerably better timing characteristics with respect to their bulk analogues [15]. However, at the preparation of SCF by the LPE method, lead ions are introduced into the crystal lattice due to the use of the PbO-based flux for the SCF growth [16]. Absorption and luminescence characteristics of Pb-related centers in the SCF of aluminium perovskites and garnets were studied in [16–19]. In [17], the spectral bands, aris-

ing from the single Pb^{2+}-based centers, were identified in LuAG SCF. It was found that the 4.75 eV band in the excitation spectrum and the 3.61 eV band in the emission spectrum arise from the electronic transitions between the ground and the triplet excited state of Pb^{2+} ions. The processes of energy transfer from the host lattice to Pb^{2+} and Ce^{3+} ions and from Pb^{2+} to Ce^{3+} ions were investigated as well. Competition between Pb^{2+} and Ce^{3+} ions in the processes of energy transfer from the LuAG crystal lattice was evidenced and found rather strong under excitation in the exciton absorption region. Due to the overlap of the 3.61 eV emission band of the single Pb^{2+}-based centers with the 3.6 eV absorption band of Ce^{3+} centers, an effective energy transfer from Pb^{2+} ions to Ce^{3+} ions takes place, resulting in the appearance of slow decay components in the luminescence of Ce^{3+} centers and a decrease of the Ce^{3+}-related luminescence intensity due to the presence of nonradiative quenching of the Pb^{2+} emission at higher temperatures.

Besides the single Pb^{2+}-based centers, more complicated lead-induced centers can also exist in SCF. The aim of the present work was to identify such lead-induced centers in the SCF of aluminium perovskites and garnets, to study their characteristics, and to clarify the influence of these centers on the luminescence characteristics of Ce^{3+} centers.

2 Experimental Single crystalline films of undoped and Ce^{3+}-doped LuAG, YAG, LuAP and YAP were prepared by the LPE method from $PbO-B_2O_3$ flux in a platinum crucible, using single crystals of LuAG, YAG or YAP as substrates (see [5, 16] and references therein). The preparation temperature T_g varied from 924 °C to 1030 °C, and the thickness H of the SCF layer from 4.1 μm to 37.5 μm. LuAG:Pb ceramics with a large Pb^{2+} content in the melt (1000 ppm, 2500 ppm and 10000 ppm) were prepared at 1130–1150 °C in a high-purity Al_2O_3 crucible and after that slowly cooled down. The luminescence characteristics were studied for the SCF with different lead concentrations (proportional to $1/T_g$) and with different total lead contents in the SCF layers (proportional also to H). The list of the samples studied in the present paper is presented in Table 1. As the SCF were grown at different SC substrates, the characteristics of these substrates were investigated as well.

The steady-state emission and excitation spectra and temperature dependences of the emission intensity were measured in the 80–350 K temperature range under selective excitation in the 2.4–6.0 eV energy range at the set-up described in [3, 17] and consisting of a deuterium DDS-400 lamp, two monochromators (SF-4 and SPM-1) and photomultiplier (FEU-39 or FEU-79) with an amplifier and recorder. The spectra were corrected for the spectral distribution of the excitation light, the transmission and dispersion of the monochromators and spectral sensitivity of the detectors used.

Luminescence decay kinetics and time-resolved emission and excitation spectra were measured at 80 K at a modified Spectrofluorometer 199S (Edinburgh Instruments) under excitation with a nanosecond coaxial hydrogen-filled flashlamp or microsecond Xe lamp (both IBH Scotland) and using two single grating monochromators. The detection was performed by an IBH-04 photomultiplier module using the method of time-correlated single photon counting. Deconvolution procedure (SpectraSolve software package) was applied to extract true decay times using the multiexponential approximation. At 10 K, the decay curves were measured under synchrotron excitation at SUPERLUMI station (HASYLAB at DESY, Hamburg, Germany). The experiments at low temperatures were carried out with the use of an immersion helium cryostat or vacuum nitrogen cryostat.

Thermally Stimulated Luminescence (TSL) measurements after X-ray irradiation (by a Machlett OEG 50 X-ray tube) were performed in the temperature range of 25–300 °C with a linear heating rate of 1 °C/s with two different apparatuses: in the first one, the total emitted light was detected as a function of temperature by photon counting technique using an EMI 9635 QB photomultiplier tube. The second one was a home-made high sensitivity TSL spectrometer, measuring the TSL intensity as a func-

Table 1 List of the samples studied. H is the thickness of the SCF layer, T_g is the SCF preparation temperature

single crystalline films			
no.	film/substrate	H	T_g
1	LuAG/LuAG	4.7 μm	1000 °C
2	LuAG/LuAG	12 μm	1005 °C
3	LuAG:Ce/LuAG	17.4 μm	995 °C
4	LuAG:Ce/LuAG	34.5 μm	1030 °C
5	LuAG:Ce/LuAG	28 μm	1030 °C
6	LuAG:Ce/YAG	4.1 μm	990 °C
7	YAG/YAG	22 μm	951 °C
8	YAG/YAG	30 μm	944.5 °C
9	YAG/YAP	11 μm	950–961 °C
10	YAG/YAP	37.5 μm	1011–1023 °C
11	YAG/YAP	16 μm	932–947 °C
12	YAG/YAP	37.5 μm	1020–1030 °C
13	YAG:Ce/YAP	55 μm	942.5 °C
14	YAG:Ce/YAP	36.5 μm	925 °C
15	YAG:Ce/YAP	35.2 μm	975 °C
16	YAP/YAP	5 μm	1018–1020 °C
17	YAP/YAP	29 μm	999–1004 °C
18	YAP/YAP	15 μm	972–985 °C
19	YAP:Ce/YAP	40 μm	1018–1026 °C
20	YAP:Ce/YAP	33 μm	956–984 °C
21	LuAP/YAP	29.5 μm	933 °C
22	LuAP:Ce/YAP	22 μm	924 °C
ceramics			
1	LuAG:1000 ppm Pb		
2	LuAG:2500 ppm Pb		
3	LuAG:10000 ppm Pb		

tion of both temperature and emission wavelength. The detector was a double stage Microchannel plate followed by a 512 diode array; the dispersive element was a 140 lines/mm holographic grating, the detection range being 1.55–6.20 eV.

3 Experimental results

3.1 Luminescence of YAP and LuAP single crystalline films According to [7, 18], a weak absorption band of YAP SCF, located at 4.97 eV, arises from the transitions into the triplet excited state of a Pb^{2+} ion. The wide (FWHM ≈ 1 eV) emission bands at 3.65 eV and 2.14 eV were both ascribed to Pb^{2+} ions. In LuAP SCF, the 5.03 eV absorption band was ascribed to Pb^{2+} ions. The emission bands of Pb^{2+} centers were concluded to be located at 3.45 eV, 3.18 eV, 2.39 eV, and 2.16 eV. The analysis of the data [7, 18] and their comparison with the results obtained by the detailed study of LuAG SCF [17] allowed us to conclude that only the UV emission band can surely be ascribed to the single Pb^{2+}-based centers. Therefore, the luminescence of single Pb^{2+}-based centers in SCF of YAP and LuAP was searched at 80 K in the 3.0–4.0 eV energy range under various selective excitations in the 4.5–5.5 eV range.

In all the samples studied (see Table 1), no clear emission band is observed in the 3.0–4.0 eV range (see, e.g., Fig. 1a and b). For this emission range, only a very weak excitation band is observed around 4.8–5.0 eV. No clear dependence of the emission intensity on the thickness of the SCF layer and on its preparation conditions (i.e. on the lead content in the layer) is found. No clear band is found in this energy range in the excitation spectrum of the Ce^{3+} emission of YAP:Ce and LuAP:Ce SCF, where this band could appear due to the $Pb^{2+} \rightarrow Ce^{3+}$ energy transfer. Thus, one can conclude that the concentration of single Pb^{2+}-based centers in the YAP and LuAP SCF studied is negligible.

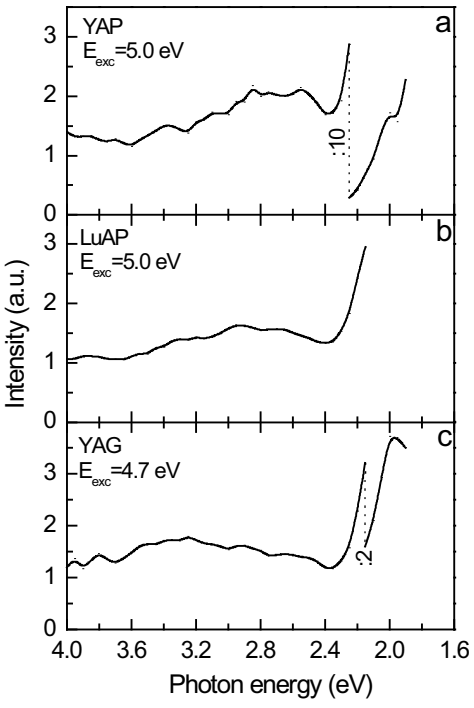

Figure 1 Emission spectra of the (a) YAP (No. 18), (b) LuAP (No. 21), and (c) YAG (No. 10) SCF measured at 80 K under excitation in the absorption band of single Pb^{2+}-based centers.

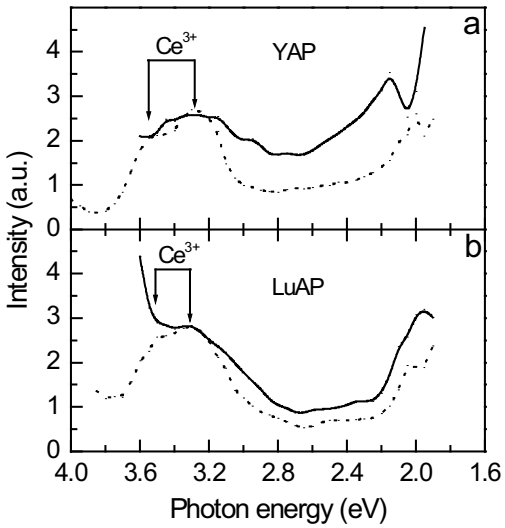

Figure 2 Emission spectra of the same (a) YAP and (b) LuAP SCF measured at 80 K under excitation at 3.8 eV (solid line) and in the Ce^{3+}-related 4.2 eV band (dotted line).

However, under excitation around 3.9 eV, a relatively intense 3.1–3.2 eV emission is observed in these SCF (Fig. 2, solid lines). This emission is strongly overlapped with the emission bands of Ce^{3+} centers, located at about 3.50 eV and 3.22 eV (dotted line), which also exist in all the samples studied. In the excitation spectrum of the

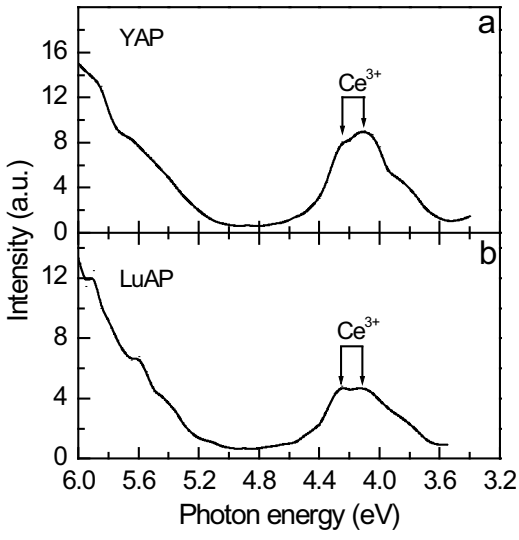

Figure 3 Excitation spectra of the same (a) YAP and (b) LuAP SCF measured for the 3.2 eV emission at 80 K.

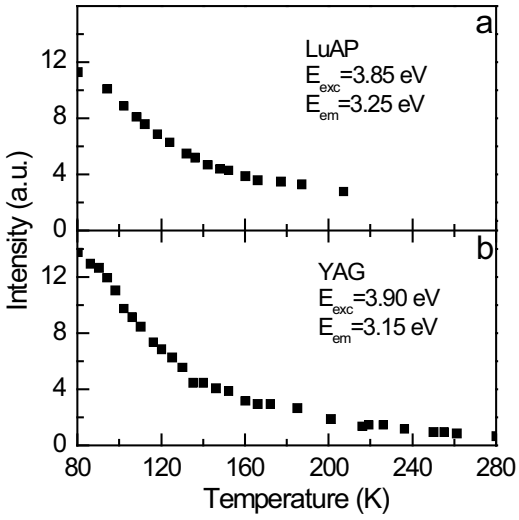

Figure 4 Temperature dependences of the ~3.2 eV emission intensity measured under 3.85–3.90 eV excitation for the (a) LuAP (No. 21) and (b) YAG (No. 8) single crystalline films.

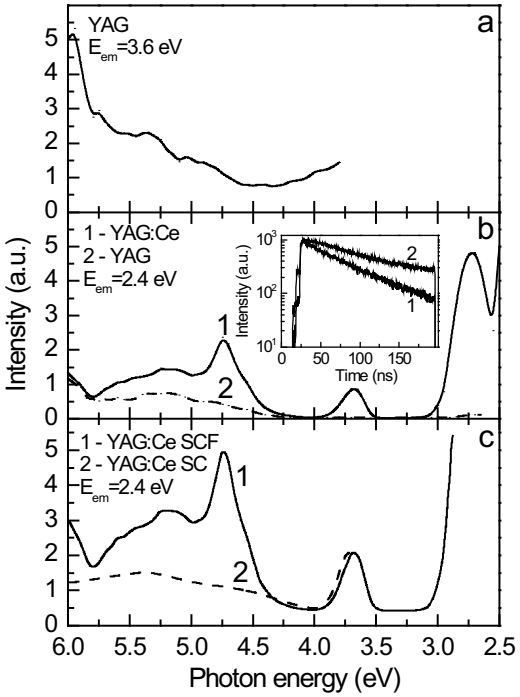

Figure 5 Excitation spectra measured at 80 K (a) for the Pb^{2+}-related 3.6 eV emission of YAG SCF No. 10, (b) for the Ce^{3+}-related 2.4 eV emission of YAG:Ce SCF No. 13 (curve 1) and YAG SCF No. 7 (curve 2), and (c) for the 2.4 eV emission of YAG:Ce SCF No. 13 (curve 1) and YAG:Ce single crystal (curve 2) with comparable Ce^{3+} contents (normalized at 3.71 eV). In the inset of Fig. 5b: the decay kinetics of the 2.4 eV emission of YAG:Ce SCF No. 13 measured at 10 K under excitation by synchrotron radiation in the Ce^{3+}-related 3.71 eV band (curve 1) and Pb^{2+}-related 4.75 eV band (curve 2).

3.1–3.2 eV emission, the characteristic 3.85–3.90 eV band appears at the low-energy side of the Ce^{3+}-related doublet excitation band consisting of the 4.25 eV and 4.10 eV components (Fig. 3). As the temperature increases, the intensity of the 3.1–3.2 eV emission decreases twice around 130 K (see, e.g., Fig. 4a). The luminescence with the mentioned characteristics is not observed in single crystals of YAP and LuAP. One may assume that in SCF it arises from lead-induced centers.

3.2 Luminescence of YAG and LuAG single crystalline films Two wide (FWHM ≈ 1 eV) emission bands around 3.3 eV and at 1.97 eV were observed at RT in the cathodoluminescence (CL) spectra of YAG:Pb SCF samples and ascribed to Pb^{2+} centers [19]. According to [19], at 10 K the UV emission band of Pb^{2+} centers is located at about 3.7 eV and excited at 4.55 eV. As the luminescence characteristics of Pb^{2+} centers in SCF of LuAG [17] and YAG should be similar, we expected to find the emission band of single Pb^{2+}-based centers in the 3.4–4.0 eV energy range and the excitation band in the 4.5–4.8 eV range.

In the YAG SCF samples No. 9–12 (see Table 1), an emission spectrum in the 3.4–4.0 eV range consists of strongly overlapped weak emission bands (see, e.g., Fig. 1c). No clear dependence of the emission intensity on the thickness of the SCF layer and on its preparation conditions (consequently, on the lead content) is found. Similar emissions are present also in the SC substrates used, and their intensity is comparable with that in SCF or it is even larger than in SCF. For this emission range, no clear excitation band is observed in the 4.5–4.8 eV energy range (see, e.g., Fig. 5a). The existence of single Pb^{2+}-based centers in YAG SCF appears only in a difference of the excitation spectra measured for the 2.4 eV emission of the Ce^{3+}-doped (No. 13) (Fig. 5b, curve 1) and undoped (No. 7) (curve 2) YAG SCF samples, namely, in the presence of the Pb^{2+}-related 4.75 eV band in the excitation spectrum of the Ce^{3+} emission, where this band appears due to the $Pb^{2+} \rightarrow Ce^{3+}$ energy transfer. Indeed, in YAG:Ce SC, this band is absent (compare curves 1 and 2 in Fig. 5c). The corresponding emission band is practically not evident due to its overlap with the Ce^{3+}-related absorption band located at about 3.7 eV. Due to the $Pb^{2+} \rightarrow Ce^{3+}$energy transfer, enabled by such an overlap, a slow decay component appears in the decay kinetics of the Ce^{3+} emission under excitation in the Pb^{2+}-related absorption band around 4.75 eV (compare curves 1 and 2 in the inset in Fig. 5b). The above-mentioned energy transfer processes were studied in detail for LuAG:Ce SCF [17]. However, the concentration of single Pb^{2+}-based centers in all the YAG SCF studied is much lower than in LuAG SCF.

A Pb-related emission band, similar to that in YAP and LuAP, is observed at 80 K in SCF of LuAG and YAG at about 3.2 eV (Fig. 6, curves 1). This emission is excited around 3.95 eV (curves 2). The FWHM of the emission band is about 0.6 eV, and the Stokes shift $S = 0.75$ eV. As the temperature increases, the intensity of the 3.2 eV emis-

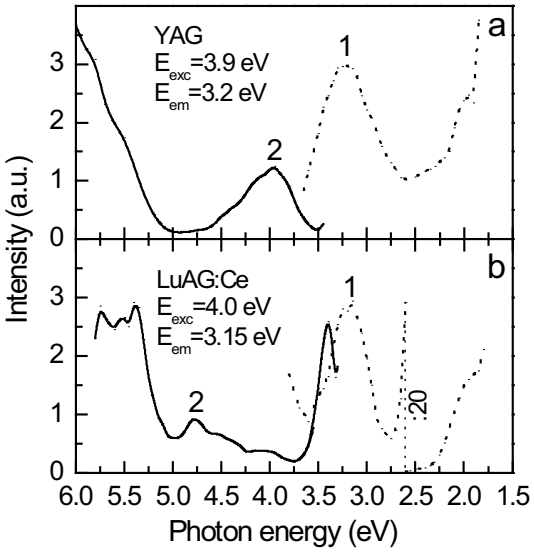

Figure 6 Emission spectra under 3.9–4.0 eV excitation and excitation spectra for the 3.15–3.20 eV emission measured at 80 K for the SCF of (a) YAG (No. 8) and (b) LuAG:Ce (No. 3).

sion in YAG decreases twice around 120 K (Fig. 4b). In LuAG SCF studied, this emission is relatively weak and strongly overlapped with an intense narrow (FWHM = 0.22 eV) emission band at 3.15 eV, which is most effectively excited around 5.5 eV and at 3.4 eV. The latter emission is present also in LuAG SC. In the decay kinetics of this emission, the fast component with $\tau = 3.14$ ns prevails at 11 K. Most probably, this emission

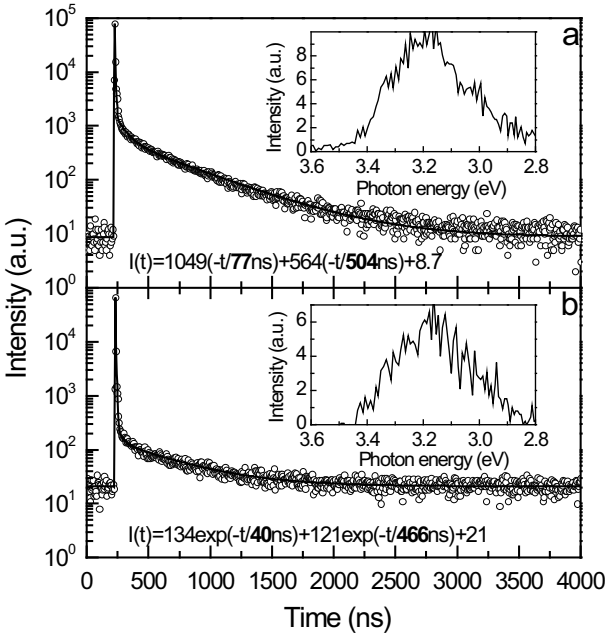

Figure 7 Luminescence decay curves measured at 80 K for the 3.15 eV emission of (a) the LuAG:1000 ppm Pb ceramics and (b) LuAG:Ce SCF No. 3. In the insets, the emission spectra of the slow decay component are shown. $E_{exc} = 3.9$ eV.

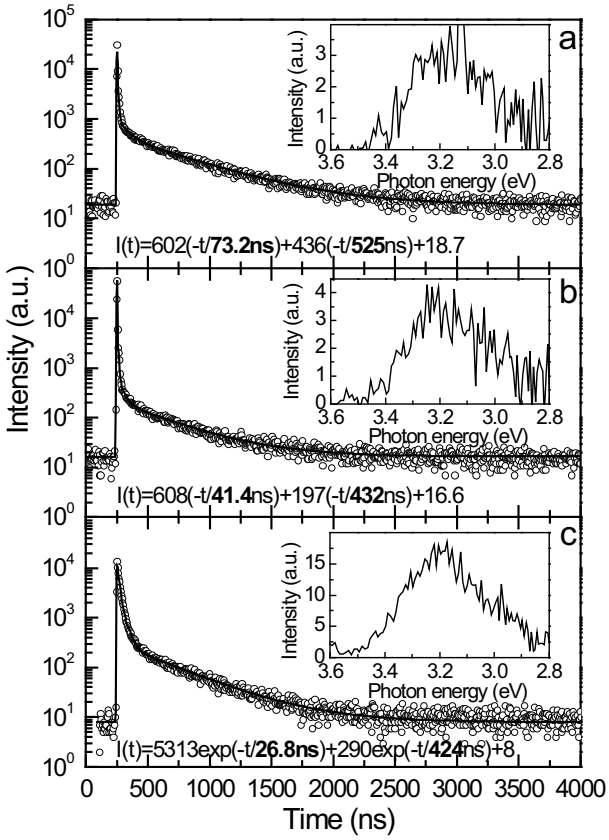

Figure 8 Luminescence decay curves measured at 80 K for the 3.15 eV emission of the SCF of (a) undoped YAG (No. 10), (b) YAG:Ce (No. 13) and (c) YAG:Pr. In the insets, the emission spectra of the slow decay component are shown. $E_{exc} = 3.95$ eV.

arises from F^+ centers [20] which points to the existence of oxygen vacancies in both SC and SCF LuAG samples under study.

Decay kinetics of the ≈3.2 eV emission is measured under 3.9 eV excitation for the undoped LuAG SCF No. 2, the LuAG:1000 ppm Pb ceramics (Fig. 7a) and LuAG:Ce SCF No. 3 (Fig. 7b). By comparing the lightsums of the fast and slow decay components, one can conclude that in all these samples, the slow component with the decay time ≈460–500 ns is the dominating one. In the decay kinetics of the ≈3.2 eV emission of undoped YAG No. 12 (Fig. 8a), YAG:Ce No. 13 (Fig. 8b) and YAG:Pr (Fig. 8c), measured under 3.95 eV excitation, the slow component with the decay time 420–525 ns is observed. The emission spectrum of this component (see the insets in Figs. 7 and 8) coincides with the emission spectrum observed at the steady-state conditions (Fig. 6). Thus, the slow decay component surely arises from the lead-induced centers. Besides the slow component, a fast component is also detected (Figs. 7 and 8). The presence of both the fast (ns) and the slow (μs-ms) components in the decay kinetics of the triplet emission is characteristics of Pb^{2+}-related centers (see, e.g., [17]). This is caused by the location of the metastable minimum under the emitting minimum in their triplet

relaxed excited state. Therefore, the weak 73–77 ns-component of the LuAG:Pb ceramics (Fig. 7a) and undoped YAG SCF (Fig. 8a) can arise from the electronic transitions from the emitting minima of the triplet excited state of the Pb^{2+} ion. In Ce^{3+}- and Pr^{3+}-doped SCF, where the decay time of the fast component is close to the decay times of the Ce^{3+} and Pr^{3+} emissions, the relatively intense fast component can mainly arise from the overlap of the ≈3.2 eV emission studied with the UV emissions of Ce^{3+} or Pr^{3+} centers (see, e.g., [3, 21]). The decay time values exhibit a continuous decrease with an increasing temperature (down to 250 ns and 50 ns at RT in the LuAG:Pb ceramics). No slow component appears in the decay kinetics of the 2.45 eV emission of Ce^{3+} under excitation in the 3.9–4.0 eV absorption region. This points to the absence of the energy transfer from the lead-induced centers to Ce^{3+} ions in the garnet lattice.

3.3 TSL of the Ce-doped YAP and LuAG above room temperature In Figs. 9 and 10, the normalized TSL glow curves of Ce-doped LuAG and YAP, both SC and SCF samples, are displayed. In all the cases, the TSL spectra consist of the usual Ce^{3+} emission peaking at 2.2–2.4 eV (LuAG:Ce) and 3.4–3.6 eV (YAP:Ce). It is worth noting the similarity of the peak positions for SC and SCF samples. Furthermore, taking into account the actual irradiation doses (notably different in both cases due to the different X-ray tube voltage applied) and experimental conditions, the absolute TSL intensity (TSL glow curve integral) for a unit irradiation dose turns out to be similar for both SC and SCF samples.

The existence of F^+ centers in the isostructural YAG host was considered to be the cause of the absorption and emission bands at 3.4 eV and 3.1 eV, respectively [20], even though no convincing evidence about oxygen vacancy-related electron traps in aluminium garnets was found e.g. in an EPR experiment [22]. In our case, the existence of oxygen vacancies in bulk Czochralski-grown SC could also be favoured by the reducing oxygen-free atmosphere used in the growth process since crystals are grown from a molybdenum crucible. The similarity of the shape and intensity of the TSL glow curves between SC and SCF samples can, thus, point to the occurrence of the same deep electron traps in both systems, and such traps are very probably related to oxygen vacancies. The same arguments can be used also in the case of perovskite samples. Moreover, the electron traps responsible for the TSL glow peaks above RT were ascribed to the oxygen vacancies in the single crystals of YAP:Ce [23] and the existence of F^+ centres in YAP was confirmed also by the EPR measurements [22]. The similarity of the peak positions in the TSL glow curves of SC and SCF systems in both the aluminium perovskites and garnets doped with Ce^{3+} demonstrates that impurity ions embedded in the samples due to the particular production technology do not give rise to electron traps. Thus, the Pb and Pt ions in the SCF films, coming from the flux and crucible, respectively, and the Mo ions in the bulk crystals, coming from the crucible, are of minor importance.

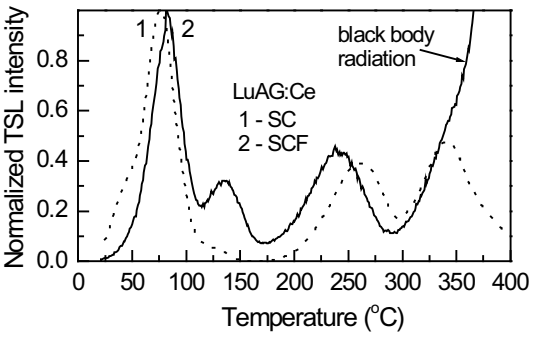

Figure 9 Normalized TSL glow curve of LuAG:Ce, single crystal (SC) and single crystalline film (SCF) samples after irradiation by an X-ray tube operated at 30 kV and 8 kV, respectively. A lower voltage was adopted in the case of SCF in order to avoid X-ray penetration in the undoped LuAG substrate.

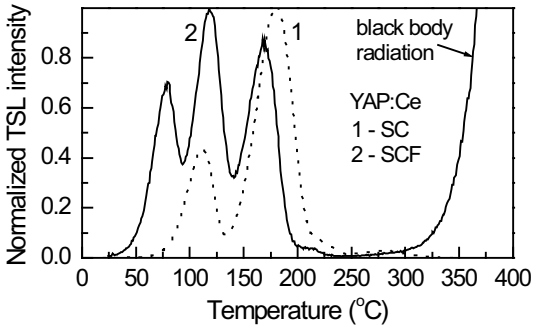

Figure 10 Normalized TSL glow curve of YAP:Ce, single crystal (SC) and 25 μm thick single crystalline film (SCF) samples after irradiation by an X-ray tube operated at 30 kV and 8 kV, respectively. A lower voltage was adopted in the case of SCF in order to avoid X-ray penetration in the undoped YAP substrate.

4 Discussion The ionic radius of a Pb^{2+} ion is large (1.29 Å) as compared with the ionic radii of the substituting Lu^{3+} (0.98 Å) or Y^{3+} (1.02 Å) ions in 8-fold coordination [24]. Besides, a Pb^{2+} ion has an effective negative charge with respect to the host crystal lattice. The charge and volume compensation can be achieved by small tetravalent impurity ions (e.g., Pt^{4+}, Pb^{4+}) or oxygen vacancies (V_O). In case Pb^{2+} ions and compensating defects are statistically distributed along the crystal lattice, single Pb^{2+} centers are mainly created. However, the close location of a Pb^{2+} ion and a compensating defect is more probable. Let us consider possible structures of Pb-related centers in the SCF studied.

4.1 Single Pb^{2+}-based centers of the type of {Pb^{2+}–Pt^{4+}} The SCF studied are grown in a platinum crucible, and due to a chemical reaction between PbO and platinum metal at high temperatures, they contain Pt ions at a concentration which can exceed the concentration of

Pb^{2+} ions. In [25], it was concluded that in this case the charge and volume of a Pb^{2+} ion in the garnet lattice are both compensated by a much smaller Pt^{4+} ion located in the Al^{3+} site, and, hence, no other defects would be necessary to compensate the Pb^{2+}, this being provided by the Pt^{4+}. However, recent ESR studies [26] have shown that trivalent Pt^{3+} ions are incorporated into the garnet lattice at a concentration of about several hundreds ppm which is comparable with the total Pt content in the SCF studied. Thus, the concentration of tetravalent Pt^{4+} ions can be small as compared with the concentration of Pb^{2+} ions. In any case, an aggregate of a single Pb^{2+} ion with a Pt ion or some other compensating defect should be considered as a *single* Pb^{2+}-based center where a Pb^{2+} ion is perturbed by the compensating defect, as the spectral bands of this center are determined by the electronic transitions between the energy levels of a Pb^{2+} ion. The luminescence characteristics of single Pb^{2+}-based centers were studied in [17].

4.2 Single Pb^{2+}-based centers of the type of $\{Pb^{2+}-Pb^{4+}\}$ In the SCF of garnets with a very large lead content, Pb^{4+} ions can also exist [25]. The Pb^{2+} and Pb^{4+} ions can be localized in dodecahedral positions of the garnet lattice, and in this case they have ionic radii 1.29 Å and 0.94 Å, respectively [24]. The sum of their ionic radii (2.33 Å) exceeds the sum of the radii of two Lu^{3+} (1.96 Å) or Y^{3+} (2.03 Å) ions, thus, the total excess volume remains uncompensated. According to [25], a wide (FWHM ≈ 1 eV) absorption band of $Y_3Ga_5O_{12}$:Pb with a large lead content, arising from the charge-transfer transitions in the ⟨111⟩-type $\{Pb^{2+}-Pb^{4+}\}$ pairs, is located in the visible spectral range (at 2.23 eV). However, no such band is detected in the YAG and LuAG SCF studied. The corresponding visible emission band has not been detected either. No other bands related to these centers are reported. One can conclude that the spectral bands located in the UV region and studied in the present paper cannot be connected with the above-mentioned ⟨111⟩-type $\{Pb^{2+}-Pb^{4+}\}$ pairs. In the $\{Pb^{2+}-Pb^{4+}\}$ associates of the type of ⟨100⟩, the influence of the Pb^{4+} ion on the Pb^{2+} ion states should be small, therefore, these centers can also be considered as *single* Pb^{2+}-based centers, where electronic transitions take place between the states of a Pb^{2+} ion perturbed by a Pb^{4+} ion. The luminescence characteristics of different single Pb^{2+}-based centers should be similar to those reported in [17] as the perturbations are weak. The small number of single Pb^{2+}-based centers in the LuAP, YAP and YAG SCF studied in the present paper (see Table 1) can be explained by the very small concentration of the Pb^{2+} ion charge and volume compensating defects (e.g., Pt^{4+} and Pb^{4+} ions) in these SCF.

4.3 Dimer $\{Pb^{2+}-V_O-Pb^{2+}\}$ centers The compensation of the Pb^{2+}-induced excess negative charge and excess volume can be achieved also by oxygen vacancies. The analysis of the TSL curves in Section 3.3 might support the existence of oxygen vacancies in SCF, despite their relatively low preparation temperature. The compensation with the aid of an oxygen vacancy V_O is the most preferable one in the case of formation of *dimer* lead centers of the type of $\{Pb^{2+}-V_O-Pb^{2+}\}$. Indeed, in such centers, two Pb^{2+} ions are located in the nearest-neighbouring dodecahedral Lu^{3+} or Y^{3+} sites separated by an oxygen vacancy V_O, and so the excess negative charge and excess volume of Pb^{2+} ion are completely compensated. Therefore, the distortion of the crystal lattice caused by this center is relatively small. Due to a strong covalent interaction between the two closely located Pb^{2+} ions, they prefer to form a quasimolecule-like $(Pb^{2+})_2$ center which should not be very sensitive to its surroundings. The characteristics of such dimer centers should differ noticeably from the characteristics of single Pb^{2+}-based centers.

Taking into account these considerations, as well as a strong difference between the characteristics of the centers responsible for the 3.1–3.2 eV emission and of single Pb^{2+}-based centers studied in [17], we assume that the 3.1–3.2 eV emission of the SCF excited around 3.90 eV arises from the dimer $\{Pb^{2+}-V_O-Pb^{2+}\}$ centers. The relatively small Stokes shift ($S = 0.7-0.8$ eV), as compared with the one that occurs in the case of the single Pb^{2+}-based centers, and the close location of the spectral bands of the dimer centers in perovskites and garnets can be explained by the relatively weak interaction of this center with its nearest environment, The decay kinetics of the 3.2 eV emission is characteristic for Pb^{2+}-related centers in LuAG [17]. Relatively small (about 0.42–0.53 μs) values of the slow component decay time as compared with that obtained at 80 K for the single Pb^{2+}-based centers (≈2 μs) can be explained by thermal quenching of the 3.2 eV emission and also by the covalent interaction between two close Pb^{2+} ions. The conclusions made are confirmed by the study of the concentration dependences of the emission intensities as well as dependences of the emission intensities on the quenching procedures carried out for the LuAG:Pb ceramics.

For the set of LuAG:Pb ceramics with a large Pb^{2+} content, the luminescence is studied at 80 K under excitation at 4.75 eV (Fig. 11a) and 3.9 eV (Fig. 11b). Due to the higher preparation temperature as compared with that used at the SCF preparation (924–1030 °C, see Table 1), these ceramics should contain a higher concentration of oxygen vacancies but they should be free from Pt. It is found that the emission and excitation spectra of single and dimer lead centers in the LuAG:1000 ppm Pb ceramics coincide with the corresponding spectra of LuAG SCF. This supports the suggestion made above that Pt ions do not influence the characteristics of the lead-induced centers studied. As the Pb^{2+} content increases, the emission intensity of both the single (near 3.6 eV, Fig. 11a) and dimer (near 3.2 eV, Fig. 11b) centers decreases. This effect can be explained by the formation of lead aggregates with the emission in the visible spectral range. Indeed, the relative intensity of the visible emission increases with the increasing lead content. From the intensity ratios shown in

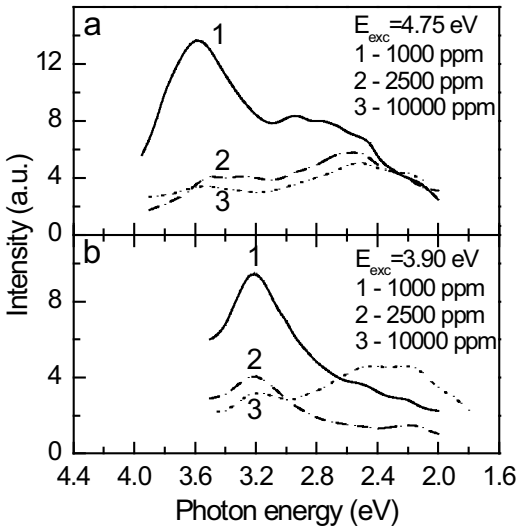

Figure 11 Emission spectra of LuAG:Pb ceramics with different lead contents (1000 ppm, 2500 ppm and 10000 ppm) measured at approximately the same conditions at 80 K under excitation (a) at 4.75 eV and (b) at 3.9 eV.

Table 2, one can see that as the lead content increases from 1000 ppm to 2500 ppm, both the 3.2 eV/3.6 eV and VIS/3.6 eV intensity ratios increase due to the transformation of single Pb^{2+}-based centers into the dimer centers and more complex aggregates. A further increase of the lead content (up to 10000 ppm) leads to the formation of lead aggregates mainly from the dimer lead centers. The aggregation process is stimulated also by the slow cooling down of the samples after their preparation.

Similar results were obtained at the study of the cathodoluminescence (CL) spectra of the SCF of YAG:Pb containing strongly different lead concentrations [19]. At RT, a wide complex UV emission band of the sample with the smallest lead content is located at 3.3 eV, i.e., it is shifted to a lower energy with respect to the ≈3.7 eV emission band of single Pb^{2+}-based centers. It means that the mentioned band is a superposition of the emission bands of the single and dimer lead centers. A wide CL band around 1.97 eV probably arises from more complex aggregates of lead ions. The increase of the lead content results in a continuous shift of the UV band to lower energies (down to 3.2 eV) due to the increase of the relative concentration of the dimer lead centers with respect to the single Pb^{2+}-based centers. At the same time, the intensity of the 1.97 eV emission increases, which indicates to the transformation of both the single and the dimer lead centers into more complex luminescent lead aggregates. A further increase of the lead concentration results in the concentration quenching of luminescence or in the formation of more complex non-luminescent lead aggregates. Indeed, the increase of the lead content leads to a drastic decrease of the CL light yield [19].

Table 2 Emission intensity ratios at 80 K in LuAG:Pb ceramics with different lead contents.

C_{Pb} (ppm)	E_{exc} = 4.75 eV			E_{exc} = 3.9 eV	
	3.2 eV/ 3.6 eV	2.5 eV/ 3.6 eV	2.2 eV/ 3.6 eV	2.5 eV/ 3.2 eV	2.2 eV/ 3.2 eV
1000	4.58	0.51	0.29	0.40	0.29
2500	6.53	1.40	0.98	0.37	0.37
10000	6.29	1.45	1.22	1.45	1.43

The quenching of the LuAG:1000 ppm Pb ceramics (by quick cooling down to RT after heating at 1000 °C for 30 min) should result in the partial transformation of dimer lead centers into single lead centers. Indeed, the increase of the 3.6 eV emission excited at 4.75 eV and decrease of the 3.2 eV emission excited at 3.9 V (up to 25%) are observed as a result of the mentioned procedure.

The very small concentration of single Pb^{2+}-based centers and the presence of dimer centers in the SCF of LuAP, YAP and YAG studied in the present paper (Table 1) may indicate that the mentioned dimer centers are more preferably produced in these SCF as compared with single Pb^{2+}-based centers.

In Ce^{3+}-doped perovskites, due to a strong overlap of spectral bands of the dimer and Ce^{3+} centers, the dimer lead centers should considerably influence the scintillation characteristics of the material. The overlap of the 3.9 eV absorption band of dimers with the Ce^{3+}-related emission band can result in the energy transfer from Ce^{3+} ions to dimer centers leading to the decrease of the Ce^{3+} emission light yield. In garnets, the influence of the dimer lead centers on the characteristics of Ce^{3+} centers is smaller as the spectral bands of Ce^{3+} centers and dimer lead centers are much less overlapped.

In all the SCF samples studied, relatively intense strongly overlapping narrow visible emission bands with the small Stokes shifts ($S = 0.3-0.5$ eV) were also observed. By analogy with LuAG SCF [17], we conclude that these bands can arise neither from single or dimer Pb^{2+} centers nor from the excitons localized near Pb^{2+} ions. In the samples with a sufficiently large lead content, they are strongly overlapped with the emission bands of lead aggregates. These bands can also arise from some other intrinsic or impurity defects introduced into SCF in the process of their preparation. Some of them arise from the SC substrate used at the preparation of the SCF.

As for the deterioration of scintillation characteristics, the dimer $\{Pb^{2+}-V_O-Pb^{2+}\}$ centers ascribed to the 3.9 eV and 3.2 eV excitation and emission bands, respectively, should be more harmful in the Ce-doped perovskite YAP- or LuAP-based materials due to the mentioned overlap of the Ce^{3+} emission and 3.9 eV dimer excitation bands. It enables an energy transfer from the $5d_1$ relaxed excited state of Ce^{3+} which decreases the quantum efficiency of the emission center itself. However, in both perovskite and garnet hosts such a center will lower the scintillation efficiency because of its low intrinsic quantum efficiency (less than 10% at RT can be deduced from Fig. 4) and enhanced

ability to trap the migrating charge carriers created under band-to-band excitation and to become the recombination center (evidenced by CL spectra).

5 Conclusions The aluminium perovskite and garnet SCF, prepared with the use of the PbO-based flux, are contaminated by lead ions. An overlap of spectral bands of lead-related and Ce^{3+} centers can lead to energy transfer processes which negatively influence scintillation characteristics. The results obtained indicate that besides the single Pb^{2+}-based centers, dimer lead centers can also exist in the SCF. In YAG, YAP and LuAP, the formation of the dimer centers is more preferable as compared with the single centers. In the perovskite SCF, the energy transfer from Ce^{3+} ions to the dimer centers will lead to a decrease of the quantum efficiency of the Ce^{3+} center. In the garnet SCF, the influence of the dimer lead centers on the Ce^{3+} centers themselves is negligible.

For the formation of lead-induced centers in aluminium perovskites and garnets, the volume and charge of Pb^{2+} ion must be compensated. In the case of the single Pb^{2+}-based centers, the compensation can be achieved by small tetravalent ions, and in the case of the dimer lead centers, by oxygen vacancies. The number of undesirable lead-induced centers in the SCF studied could be reduced by the decrease of the concentration of the corresponding compensating defects.

Acknowledgements This work was partly supported by the Estonian Science Foundation project No. 7507, the project of Czech Science Foundation No. 202/08/0893, and the project of the Ukrainian Ministry of Education and Science No. SF-77 F.

References

[1] A. Lempicki, M. H. Randles, D. Wisniewski, M. Balcerzyk, C. Brecher, and A. J. Wojtowicz, IEEE Trans. Nucl. Sci. **42**, 280 (1995).
[2] M. Nikl, E. Mihokova, J. A. Mares, A. Vedda, M. Martini, K. Nejezchleb, and K. Blazek, Phys. Status Solidi B **181**, R10 (2000).
[3] K. Blazek, A. Krasnikov, K. Nejezchleb, M. Nikl, T. Savikhina, and S. Zazubovich, Phys. Status Solidi B **241**, 1134 (2004).
[4] M. J. Weber, Solid State Commun. **12**, 741 (1973).
[5] Yu. Zorenko, V. Gorbenko, A. Voloshinovskii, G. Stryganyuk, V. Mikhailin, V. Kolobanov, D. Spassky, M. Nikl, and K. Blazek, Phys. Status Solidi A **202**, 1113 (2005).
[6] V. Babin, K. Blazek, A. Krasnikov, K. Nejezchleb, M. Nikl, T. Savikhina, and S. Zazubovich, Phys. Status Solidi C **1**, 97 (2005).
[7] Yu. Zorenko, A. Voloshinovskii, V. Gorbenko, T. Zorenko, M. Nikl, and K. Nejezchleb, Phys. Status Solidi C **4**, 963 (2007).
[8] Yu. Zorenko, V. Gorbenko, I. Konstankevych, A. Voloshinovskii, G. Stryganyuk, V. Mikhailin, V. Kolobanov, and D. Spassky, J. Lumin. **114**, 85 (2005).
[9] M. M. Kuklja, J. Phys.: Condens. Matter **12**, 2953 (2000).
[10] C. R. Stanek, K. J. McClellan, M. R. Levy, and R. W. Grimes, Phys. Status Solidi B **243**, R75 (2006).
[11] C. R. Stanek, K. J. McClellan, M. R. Levy, C. Milanese, and R. W. Grimes, Nucl. Instrum. Methods Phys. Res. A **579**, 27 (2007).
[12] C. R. Stanek, K. J. McClellan, M. R. Levy, and R. W. Grimes, J. Appl. Phys. **99**, 113518 (2006).
[13] D. J. Singh, Phys. Rev. B **76**, 214115 (2007).
[14] M. Nikl, Phys. Status Solidi A **202**, 201 (2005).
[15] P. Prusa, T. Cechak, J. A. Mares, M. Nikl, A. Beitlerova, N. Solovieva, Yu. V. Zorenko, V. I. Gorbenko, J. Tous, and K. Blazek, Appl. Phys. Lett. **92**, 041903 (2008).
[16] Yu. Zorenko, Opt. Spectrosc. **100**, 572 (2006).
[17] V. Babin, V. Gorbenko, A. Makhov, J. A. Mares, M. Nikl, S. Zazubovich, and Yu. Zorenko, J. Lumin. **127**, 384 (2007).
[18] Yu. Zorenko, V. Gorbenko, E. Mihokova, M. Nikl, K. Nejezchleb, A. Vedda, V. Kolobanov, and D. Spassky, Radiat. Meas. **42**, 528 (2007).
[19] Yu. Zorenko, V. Gorbenko, T. Voznyak, and T. Zorenko, Phys. Status Solidi B **245**, 1618 (2008).
[20] M. Springis, A. Pujats, and J. Valbis, J. Phys.: Condens. Matter **3**, 5457 (1991).
[21] H. Ogino, A. Yoshikawa, M. Nikl, A. Krasnikov, K. Kamada, and T. Fukuda, J. Cryst. Growth **287**, 335 (2006).
[22] M. Nikl, V. V. Laguta, and A. Vedda, Phys. Status Solidi B **245**, 1702 (2008).
[23] A. Vedda, M. Martini, F. Meinardi, J. A. Mares, E. Mihokova, J. Chval, M. Dusek, and M. Nikl, Phys. Rev. B **61**, 8081 (2000).
[24] M. J. Weber, Handbook of Optical Materials (CRC Press, Boca Raton, 2003).
[25] G. B. Scott and J. L. Page, J. Appl. Phys. **48**, 1342 (1977).
[26] V. V. Laguta, A. M. Slipenyuk, M. D. Glinchuk, I. P. Bykov, Yu. Zorenko, M. Nikl, J. Rosa, and K. Nejezchleb, Radiat. Meas. **42**, 835 (2007).

